

# Comparison of OTDMA and Synchronous OCDMA with Optical and Electrical Decoding

Robert Fritsch, Joachim Speidel

Institut für Nachrichtenübertragung, Universität Stuttgart, Pfaffenwaldring 47, D-70469 Stuttgart  
 {fritsch, speidel}@inue.uni-stuttgart.de

**Abstract**— For upstream digital communication in a Passive Optical Network (PON) three synchronous multiple access schemes are investigated: Optical TDMA (OTDMA) and optical CDMA (OCDMA) with Walsh Hadamard Codes and Perfect Difference Codes. We propose an improved scheme for OCDMA which employs dedicated signature sequences for bit 0 and bit 1 allowing for differential decoding at the receiver with minimum multi user interference (MUI) in the optical signal. The performance of these methods in the presence of additive white Gaussian noise is compared with respect to bit error probability and number of users. Both, optical and electrical decoders are considered. As a result, OTDMA is superior to the other solutions with optical decoders. This also holds, if electrical decoders are used. Our proposed Walsh Hadamard Code outperforms the Perfect Difference Code in case of a small number of transmitters.

**Keywords**—OCDMA, OTDMA, Performance Analysis

## I. INTRODUCTION

FOR upstream communication in a Passive Optical Network (PON) in Fig. 1 the access can be done by Time Division Multiple Access (TDMA), Code Division Multiple Access (CDMA) or Wavelength Division Multiple Access (WDMA). In case of CDMA synchronous or asynchronous transmission is possible [1], [2], [3]. In this paper we focus on bit synchronous CDMA. In the following the optical network units (ONU) are called transmitter (tx).

Each bit  $a_{\nu,k} \in \{0, 1\}$  of transmitter  $\nu$  at time  $k$  is spread into a chip pattern

$$\vec{c}_{\nu,i} = (c_{\nu,i,1}, c_{\nu,i,2}, \dots, c_{\nu,i,n})^T, \quad (1)$$

with  $i = a_{\nu,k} \in \{0, 1\}$ ,  $c_{\nu,i,m} \in \{0, 1\}$ ,  $\nu$  and  $m = 1, 2, \dots, n$ . The chip pattern is often called signature sequence or CDMA codeword.  $n$  is the number of transmitters which is in this paper equal to the number of chips of the CDMA codewords.  $n = \frac{T_b}{T_c}$  is also called spreading factor, where  $T_b$  and  $T_c$  is the bit and chip duration, resp.  $b_\nu(t)$  is the output of tx  $\nu$ . The received signal at the input of the head end is  $u(t)$ . For simplicity reasons we assume, that the fiber connection from the output of tx  $\nu$  to the input of the head end is characterized only by the attenuation  $\alpha_{\text{PON},\nu} \geq 1$ . So, dispersion effects are assumed to be

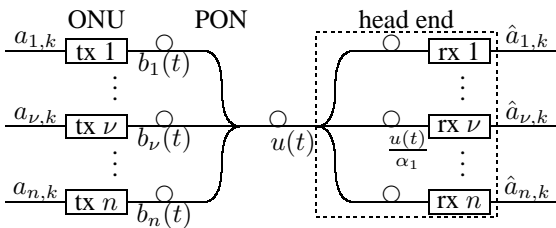


Fig. 1. Principal communication system (tx transmitter, rx receiver)

properly compensated. It is important to note, that the power of each transmitter signal  $b_\nu(t)$  ( $\nu = 1, 2, \dots, n$ ) is adjusted such that it arrives with the same power  $\frac{P_1}{n}$  at the head end. This means, that the near-far-problem [4] is solved by compensation of  $\alpha_{\text{PON},\nu}$  individually for each tx  $\nu$ . The average power of  $u(t)$  at the input of the head end then is  $n \cdot \frac{P_1}{n} = P_1$ . The optical power signal  $u(t)$  is split into  $n$  parts, which provide the same input signal  $\frac{u(t)}{\alpha_1}$  for each receiver rx  $\nu$  ( $\nu = 1, 2, \dots, n$ ). In Fig. 1,  $\alpha_1 = n$  holds. The receiver detects the input signal and outputs an estimate  $\hat{a}_{\nu,k}$  of the transmitted bit sequence  $a_{\nu,k}$ . O/E-conversion is done in each rx.

The principal structure of the  $\nu$ th transmitter is depicted in Fig. 2 and consists of two paths, which spread bit “0” and bit “1” into different codewords to allow for differential decoding at the receiver. This is done to overcome the problem, that to the codewords for bit “0” and bit “1” no negative impulses can be allocated to, as for electrical CDMA, because the optical power signal can only be positive. In the upper path bits  $a_{\nu,k} = 1$  are coded with the codeword  $\vec{c}_{\nu,1}$ . Therefore the value  $a_{\nu,k}$  is mapped to an impulse  $g_{\nu,1}(t - kT_b)$ , if  $a_{\nu,k} = 1$ . At the lower path bits  $a_{\nu,k} = 0$  are coded with the codeword  $\vec{c}_{\nu,0}$ . Therefore bit  $a_{\nu,k}$  is negated to  $\bar{a}_{\nu,k} = (1 - a_{\nu,k})$  at the beginning of the lower path and mapped to the impulse  $g_{\nu,0}(t - kT_b)$ . Thus, the optical output power signal of the  $\nu$ th transmitter is

$$b_\nu(t) = \frac{\alpha_{\text{PON},\nu} P_1}{w} \sum_{k=-\infty}^{\infty} g_{\nu,a_{\nu,k}}(t - kT_b). \quad (2)$$

Mean output power of each tx depends on the number of 1-chips within a spreading code (1). As we would like to compare different codes on a fair basis, a factor  $w$  which depends on the selected code ensures the same mean transmit power for all codes. The bit impulses  $g_{\nu,i}(t)$ ,  $i = 0, 1$  consist of delayed chip impulses  $g(t)$ . For simplicity,  $g(t)$  is a rectangular impulse with  $g(t) = 1$  for  $0 < t < T_c$  and  $g(t) = 0$  outside.

$$g_{\nu,i}(t) = \sum_{j=1}^n c_{\nu,i,j} \cdot g(t - (j-1)T_c) \quad (3)$$

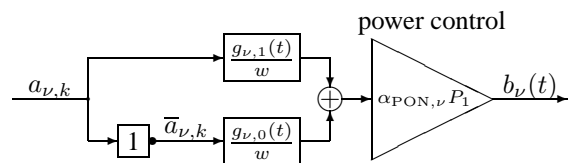


Fig. 2. Principal structure of transmitter tx  $\nu$

Thus, the input signal  $u(t)$  of the head end is

$$u(t) = \frac{P_1}{w} \sum_{\mu=1}^n \sum_{k=-\infty}^{\infty} \sum_{j=1}^n c_{\mu, a_{\mu, k}, j} \cdot g(t - (j-1)T_c - kT_b). \quad (4)$$

Note, if all tx in Fig. 1 transmit bits  $a_{\nu, k}$  with equal probability,  $u(t)$  exhibits the mean power  $P_1$ . This assumption is made throughout this paper.

In Fig. 3. the principal structure of the  $\nu$ th receiver is shown. As mentioned earlier,  $\alpha_1$  is the attenuation of the splitter at the beginning of the head end. The differential optical receiver  $\nu$  splits its optical input signal  $\frac{u(t)}{\alpha_1}$  into two branches. Thus, an additional attenuation  $\alpha_2$  is introduced. The total attenuation is

$$\alpha = \alpha_1 \cdot \alpha_2.$$

Obviously, rx  $\nu$  is a correlation receiver. Its structure is very convenient as a mathematical model. Normally, it cannot be implemented directly with optical components, because multiplication is not very feasible. However, as is well known from theory, a correlation receiver can be replaced by an equivalent matched filter receiver. Such a solution will be given later in Fig. 5. The signal  $d_{\nu}(t)$  at the input of the sampler is

$$\begin{aligned} d_{\nu}(t) &= \int_{\xi=t-T_b}^t \frac{S_S}{\alpha T_c} u(\xi) \sum_{k=-\infty}^{\infty} g_{\nu,1}(\xi - kT_b) d\xi \\ &\quad - \int_{\xi=t-T_b}^t \frac{S_S}{\alpha T_c} u(\xi) \sum_{k=-\infty}^{\infty} g_{\nu,0}(\xi - kT_b) d\xi \\ &= \frac{P_1 S_S}{\alpha w T_c} \int_{\xi=t-T_b}^t \sum_{\mu=1}^n \sum_{k=-\infty}^{\infty} \sum_{j=1}^n c_{\mu, a_{\mu, k}, j} (c_{\nu,1,j} - c_{\nu,0,j}) \\ &\quad \cdot g^2(\xi - (j-1)T_c - kT_b) d\xi \end{aligned}$$

$S_S$  is the photo sensitivity of the avalanche photo diode (APD) (see later). The signal at the output of the sampler at discrete time  $t = (k+1)T_b$  is

$$d_{\nu, k} = \frac{P_1 S_S}{\alpha w T_c} \sum_{\mu=1}^n \sum_{j=1}^n c_{\mu, a_{\mu, k}, j} \underbrace{(c_{\nu,1,j} - c_{\nu,0,j})}_0 \int_{\xi=t-T_b}^t g^2(t) dt. \quad (5)$$

For optical CDMA, the coder is often implemented as an FIR filter with the coefficient vector  $\vec{c}_{\nu, i}$ , eg. by optical delay lines. This also holds for the correlation at the receiver which is often implemented with optical matched FIR filter with coefficients, which are arranged in visa versa order [5].

Aim of this work is to investigate the bit error probability as a function of the signal-to-noise ratio for OTDMA and OCDMA using different codes. Both, optical and electrical decoders are compared.

## II. CODES

In this paper we consider three codes listed in Table I: The TDM Code (TDMC), as a special case of a CDMA code, the

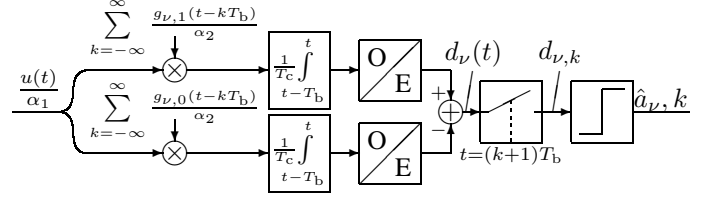


Fig. 3. Model of receiver  $\nu$

TABLE I  
CODES FOR SYNCHRONOUS OCDMA

TDM Code			Walsh Hadamard Code			Perf. Diff. Code				
$n$	$\nu$	$\vec{c}_{\nu,1}$	$n$	$\nu$	$\vec{c}_{\nu,1}$	$\vec{c}_{\nu,0}$	$n$	$\nu$	$\vec{c}_{\nu,1}$	
2	1	10	2	1	11	00	3	1	110	
	2	01		2	10			01	2	101
3	1	100	4	1	1111	0000	7	1	1101000	
	2	010		2	1010			0101	2	1010001
	3	001		3	1100			0011	3	0100011
4	1	1000	8	1	11111111	00000000	4	1	1000110	
	2	0100		2	10101010			01010101	5	0001101
	3	0010		3	11001100			00110011	6	0011010
	4	0001		4	10011001			01100110	7	0110100
5	1	10000	5	1	11110000	00001111				
	2	01000		2	10100101			01010101		
	3	00100		3	11000011			00111100		
	4	00010		4	10010110			01101001		
	5	00001		5	10010110			01101001		

Walsh Hadamard Code (WHC) [6] and the Perfect Difference Code (PDC) [7]. The length  $n$  of the codewords and the number  $n$  of transmitters per code is equal. For simplicity we assume that all users send bit “0” and bit “1” with the same a priori probability.

### A. TDM Code (TDMC)

Synchronous CDMA includes TDMA as a special case. In this case we call the signature sequence  $\vec{c}_{\nu, i}$  “TDM Code”. As the coder in Fig. 2 operates in the optical domain, this multiplexing technique can also be referred to as Optical TDM (OTDM).

TDMC has the property, that only the chip  $c_{\nu,1,\nu}$  in the codeword  $\vec{c}_{\nu,1}$  (1) is equal to 1 and all other chips are 0. In terms of OTDM, the position of the “1” chip defines the time slot of the transmitter. Thus, the received signal  $d_{\nu, k}$  contains no multi user interference (MUI), because bit “0” is encoded with  $\vec{c}_{\nu,0} = \vec{0}$ ,  $\nu = 1, 2, \dots, n$  and  $\vec{c}_{\nu,1} \perp \vec{c}_{\mu,1} \Leftrightarrow \vec{c}_{\nu,1}^T \cdot \vec{c}_{\mu,1} = 0$ ,  $\nu \neq \mu$ ,  $\nu, \mu = 1, 2, \dots, n$ .

For TDMC  $w = \frac{1}{2}$  and we get from (5)

$$d_{\nu, k} = \frac{2P_1 S_S}{\alpha} \cdot \vec{c}_{\nu, a_{\nu, k}}^T \cdot \vec{c}_{\nu,1} = \frac{2P_1 S_S}{\alpha} \cdot a_{\nu, k}. \quad (6)$$

### B. Walsh Hadamard Code (WHC)

WHC in Tab. I shows the property, that  $\vec{c}_{\nu,1}$  is the inverse of  $\vec{c}_{\nu,0}$ . With  $w = \frac{n}{2}$  we obtain from (5)

$$d_{\nu, k} = \frac{2P_1 S_S}{n\alpha} \begin{cases} (n-1) \cdot \frac{n}{2} + a_{1,k} \cdot n & \nu=1 \\ -\frac{n}{2} + a_{\nu,k} \cdot n & \nu=2,3,\dots,n \end{cases}$$

$$= \frac{2P_1 S_S}{\alpha} \cdot a_{\nu,k} - \frac{P_1 S_S}{\alpha} + \begin{cases} n \frac{P_1 S_S}{\alpha} & \nu=1 \\ 0 & \nu=2, \dots, n \end{cases} \quad (7)$$

Obviously,  $d_{\nu,k}$  does not contain bits  $a_{\mu,k}$  of other users  $\mu \neq \nu$ , so it is free of MUI, just a constant level is added. This is surprising on the first glance, because with some exceptions the  $\vec{c}_{\nu,i}$  are not orthogonal. The reason why no MUI is present lies in the differential structure of the receiver, which we propose in Fig. 3. As a consequence, the resulting  $\vec{c}_{\nu,1} - \vec{c}_{\nu,0}$ ,  $\nu = 2, 3, \dots, n$  are bipolar versions of Walsh Hadamard codewords which are orthogonal to  $\vec{c}_{\mu,i}$ ,  $i = 1, 2$ ;  $\mu = 1, 2, \dots, n$ ;  $\mu \neq \nu$ . Only  $\vec{c}_{1,1} - \vec{c}_{1,0} = \vec{c}_{1,1}$  remains unipolar. But this does not matter, because  $\vec{c}_{\mu,i}^T \cdot \vec{c}_{1,1} = \frac{n}{2} = \text{const.}$ ,  $\mu = 2, 3, \dots, n$ , independent of  $i$ . Thus, only the decision threshold has to be adjusted properly at the rx in Fig. 3. The eye opening  $\frac{2P_1 S_S}{\alpha}$  is the same as for the system with TDMC.

### C. Perfect Difference Code (PDC)

PDC are discussed in detail in [7]. However, in [7] the power at the input of each of the  $n$  receivers in Fig. 1 is kept constant. Recall, that in our consideration, the input power at the head end is kept constant. So, we take the power splitters of the head end into account, to provide a fair comparison of the different proposals. Thus, the results differ in this respect. Furthermore,  $w$  is given by

$$w = \frac{\sqrt{4n-3} + 1}{4}. \quad (8)$$

Without details of the calculation, we obtain

$$d_{\nu,k} = \frac{2P_1 S_S (\sqrt{4n-3} - 1)}{\alpha \alpha_3 (\sqrt{4n-3} + 1)} \cdot a_{\nu,k}. \quad (9)$$

with  $\alpha = \alpha_1 \cdot \alpha_2$  and

$$\alpha_3 = 1 + \frac{2r}{\sqrt{4n-3} + 1}. \quad (10)$$

$\alpha_3$  is an additional attenuation of the upper path and  $r$  is a parameter of the lower path of the receiver, [7].

### III. BIT ERROR PROBABILITY WITH OPTICAL RECEIVER

For O/E conversion an electronic receiver with Avalanche Photodiode (APD) shall be used. Transmitted bits “0” and “1” have equal a priori probabilities. The output  $d_{\nu,k}$  of the receiver in Fig. 3 is now considered to be corrupted by additive noise of the APD and thermal noise of the load resistor  $R_L$ . The total noise is assumed to be white gaussian with zero mean. As the target of our investigation is the impact of noise on the bit error probability, fiber optic transmission is considered to be linear and with no intersymbol interference.

The power density spectrum (PDS) of the noise is assumed to be

$$S_o(f) = e \left( \underbrace{\left( I_D + \frac{\eta \lambda e}{hc} p_{\nu,k} \right) M^2 F_M}_{\text{from APD}} + \underbrace{\frac{2k_B T_r}{R_L}}_{\text{from } R_L} \right). \quad (11)$$

The parameters are listed in Table II.  $p_{\nu,k}$  is the received optical power. We model the optical receiver as an ideal low pass filter

TABLE II  
PARAMETERS OF O/E CONVERTER AT RECEIVER

Name	Symbol	Value
Wavelength of the light source	$\lambda$	1300 nm
APD quantum efficiency	$\eta$	0.6
APD gain	$M$	100
APD leakage current	$I_D$	0.1 nA
chip duration	$T_c$	0.1 ns
Receiver noise temperature	$T_r$	350 K
Receiver load resistor	$R_L$	1000 $\Omega$
Planck's constant	$h$	$6.6260755 \cdot 10^{-34}$ Js
Boltzmann's constant	$k_B$	$1.380658 \cdot 10^{-23} \frac{J}{K}$
Electron charge	$e$	$1.60217733 \cdot 10^{-19}$ As
speed of light	$c$	$2.9972458 \cdot 10^8 \frac{m}{s}$
Excess noise factor	$F_M$	$M^{0.3}$
photo sensitivity	$S_S$	$M \frac{\eta \lambda e}{hc}$

with the cut-off frequency  $f_c = \frac{1}{T_c}$  and gain 1. Then we get the variance of the additive gaussian noise

$$\sigma^2 = \int_{-f_c}^{f_c} S_o(f) df = \frac{2e}{T_c} (I_D + \frac{\eta \lambda e}{hc} p_{\nu,k}) M^2 F_M + \frac{4k_B T_r}{R_L T_c}. \quad (12)$$

### A. TDM Codes

The lower path of the receiver in Fig. 3 can be dropped for TDMC, because  $\vec{c}_{\mu,0} = \vec{0}$ ,  $\mu = 1, 2, \dots, n$ . From (6) the power signal at the input of the APD in the upper path is

$$p_{\nu,k} = \frac{2P_1}{\alpha} \cdot a_{\nu,k}. \quad (13)$$

Thus, if we replace  $p_{\nu,k}$  in (12) by (13) we get the noise variance

$$\sigma_{a_{\nu,k}}^2 = \frac{2e}{T_c} \left( I_D + \frac{\eta \lambda e}{hc} \frac{2P_1}{\alpha} a_{\nu,k} \right) M^2 F_M + \frac{4k_B T_r}{R_L T_c} \quad (14)$$

which depends on the bits  $a_{\nu,k}$ . A straightforward calculation yields the mean bit error probability of each user

$$P_b = \frac{1}{2} \left[ Q \left( \frac{\frac{2P_1 S_S}{\alpha} - E}{\sigma_1} \right) + Q \left( \frac{E}{\sigma_0} \right) \right] \quad (15)$$

with the optimal decision threshold  $E$  for minimum  $P_b$

$$E = \frac{\sqrt{\sigma_0^2 \sigma_1^2 \left[ \left( \frac{2P_1 S_S}{\alpha} \right)^2 + 2(\sigma_1^2 - \sigma_0^2) \ln \frac{\sigma_1}{\sigma_0} \right]} - \left( \frac{2P_1 S_S}{\alpha} \right) \sigma_0^2}{\sigma_1^2 - \sigma_0^2}. \quad (16)$$

and

$$Q(\alpha) = \frac{1}{\sqrt{2\pi}} \int_{\alpha}^{\infty} e^{-\frac{u^2}{2}} du \quad (17)$$

the Q-function.

## B. Walsh-Hadamard Codes

Both paths of the receiver in Fig. 3 are in use. Thus, there are two statistically independent noise sources. As is well known, their power density spectra are added by the summing node in Fig. 3. First, we have to calculate the input power signals of the two APDs and then the PDS. For the upper (u) branch in Fig. 3 we get

$$p_{\nu,k}^{(u)} = \frac{P_1}{\alpha \frac{n}{2}} \cdot \begin{cases} \underbrace{\frac{(n-1)n}{2}}_{\text{from user } \mu=2,\dots,n} + \underbrace{na_{1,k}}_{\text{from user 1}} & \nu=1 \\ \underbrace{\frac{(n-2)n}{4}}_{\text{from user } \mu=2,\dots,n, \mu \neq \nu} + \underbrace{\frac{n}{2}a_{1,k}}_{\text{from user 1}} + \underbrace{\frac{n}{2}a_{\nu,k}}_{\text{from user } \nu} & 2 \leq \nu \leq n \end{cases} \quad (18)$$

$$S_o^{(u)}(f) = e \left( I_D + \frac{\eta \lambda e}{hc} p_{\nu,k}^{(u)} \right) M^2 F_M. \quad (19)$$

For the lower (l) branch we obtain

$$p_{\nu,k}^{(l)} = \frac{P_1}{\alpha \frac{n}{2}} \cdot \begin{cases} 0 & \nu=1 \\ \underbrace{\frac{(n-2)n}{4}}_{\text{from user } \mu=2,\dots,n, \mu \neq \nu} + \underbrace{\frac{n}{2}a_{1,k}}_{\text{from user 1}} + \underbrace{\frac{n(1-a_{\nu,k})}{2}}_{\text{from user } \nu} & 2 \leq \nu \leq n \end{cases} \quad (20)$$

$$S_o^{(l)}(f) = e \left( I_D + \frac{\eta \lambda e}{hc} p_{\nu,k}^{(l)} \right) M^2 F_M. \quad (21)$$

Summing up the power density spectra of the noise currents of the two APDs, we obtain

$$S_o^{(\text{APDs})}(f) = e \left( 2I_D + \frac{\eta \lambda e}{hc} \cdot \underbrace{\frac{P_1}{\alpha} ((n-1) + 2a_{1,k})}_{p_{\nu,k}^{(u)} + p_{\nu,k}^{(l)}} \right) M^2 F_M. \quad (22)$$

As can be seen, (22) depends only on the bits  $a_{1,k}$  of user 1. We now assume, that we have only one amplifier for both O/E-converters in Fig. 3, which also implements the summation and which is modelled as ideal low pass filter with gain 1, cut-off frequency  $f_c = \frac{1}{T_c}$  and with resistor load  $R_L$ . Hence

$$S_o^{(R_L)} = \frac{2k_B T_r}{R_L} \quad (23)$$

is the power density spectrum of the third noise source. We get the total noise variance of each receiver  $\nu = 1, 2, \dots, n$

$$\begin{aligned} \sigma_{a_{1,k}}^2 &= \int_{-f_c}^{f_c} \left[ S_o^{(\text{APDs})}(f) + S_o^{(R_L)}(f) \right] df \\ &= \frac{2e}{T_c} \left[ 2I_D + P_1 \frac{\eta \lambda e}{hc} \left( \frac{2}{\alpha} a_{1,k} + \frac{n-1}{\alpha} \right) \right] M^2 F_M + \frac{4k_B T_r}{R_L T_c}. \end{aligned} \quad (24)$$

Thus, the mean bit error probability of each receiver of an OCDMA system with WHC is

$$P_b = \frac{1}{2} \left[ Q \left( \frac{\frac{2P_1 S_s}{\alpha} - E}{\sigma_1} \right) + Q \left( \frac{E}{\sigma_0} \right) \right] \quad (25)$$

with the optimal decision threshold  $E$  for minimum  $P_b$  according to (16) with  $\sigma_0$  and  $\sigma_1$  given in (24).

## C. Perfect Difference Codes

Similar to the calculation of  $P_b$  for WHC we obtain without details the power density spectrum

$$S_o^{(\text{APDs})}(f) = e M^2 F_M \left( 2I_D + \frac{\eta \lambda e}{hc} \cdot \frac{P_1}{\alpha} \frac{8I_k + (2\sqrt{4n-3}+6)a_{\nu,k}}{2r + \sqrt{4n-3}+1} \right). \quad (26)$$

where

$$I_k = \sum_{\substack{\mu=1 \\ \mu \neq \nu}}^n a_{\mu,k} \quad (27)$$

is the number of other users ( $\mu \neq \nu$ ) sending bit "1". This leads to the noise variance

$$\begin{aligned} \sigma_{a_{\nu,k}}^2(I_k) &= \frac{4k_B T_r}{R_L T_c} + \frac{2e}{T_c} M^2 F_M \left[ 2I_D + \frac{\eta \lambda e}{hc} \cdot \frac{P_1}{\alpha} \frac{8I_k + (2\sqrt{4n-3}+6)a_{\nu,k}}{2r + \sqrt{4n-3}+1} \right]. \end{aligned} \quad (28)$$

The bit error probability of each receiver of an OCDMA system with PDC with  $n$  users is

$$P_b = \sum_{i=0}^{n-1} \binom{n-1}{i} \left( \frac{1}{2} \right)^n \left[ Q \left( \frac{\frac{2P_1 S_s (\sqrt{4n-3}-1)}{\alpha \alpha_3 (\sqrt{4n-3}+1)} - E}{\sigma_1(i)} \right) + Q \left( \frac{E}{\sigma_0(i)} \right) \right]. \quad (29)$$

## IV. BIT ERROR PROBABILITY WITH ELECTRICAL RECEIVER

If the head end converts the optical signal at the input into an electrical signal, no optical splitters are necessary. If an A/D converter follows the O/E converter and the remaining functions are done digitally, the attenuation  $\alpha = \alpha_1 \cdot \alpha_2 = 1$ . Thus for TDMC and WHC the results above can be used with  $\alpha = 1$ .

Only in case of PDC we assume a different receiver with the principal structure depicted in Fig. 4. As  $\vec{c}_{\nu,0}$  is equal to the inverted codeword  $\vec{c}_{\nu,1}$ ,  $g_{\nu,0}$  is given with (3) by

$$g_{\nu,0}(t) = \sum_{j=1}^n (1 - c_{\nu,1,j}) \cdot g(t - (j-1)T_c) \quad (30)$$

As can be seen from Tab. I, each codeword  $\vec{c}_{\nu,1}$  of a PDC consists of  $2w$  1-chips and  $\vec{c}_{\mu,1}^T \cdot \vec{c}_{\nu,1} = 1$  with  $\mu \neq \nu$  holds.  $w$  is given in (8). Thus, the 1-chip positions of the considered receiver  $\nu$  are disturbed by  $I_k$  and the 0-chip positions by

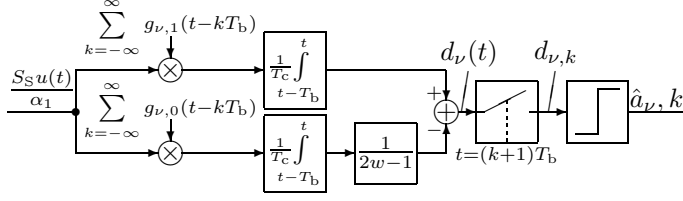


Fig. 4. principal structure of receiver  $\nu$  for PDC

$I_k \cdot (2w - 1)$ . Hence the signal at the output of the sampler at discrete time  $t = (k + 1)T_b$  in Fig. 4 is

$$d_{\nu,k} = \frac{P_1 S_S}{\alpha w} \left[ \underbrace{2w a_{\nu,k} + I_k}_{\text{upper path}} - \underbrace{\frac{I_k (2w - 1)}{2w - 1}}_{\text{lower path}} \right] = \frac{2P_1 S_S}{\alpha} a_{\nu,k}.$$

The eye opening is  $\frac{2P_1 S_S}{\alpha}$  and is the same as for the system with TDMC.

With the noise variance

$$\sigma_{a_{\nu,k}}^2(I_k) = \frac{4k_B T_r}{R_L T_c} + \frac{2e}{T_c} M^2 F_M \left[ 2I_D + \frac{\eta \lambda e}{hc} \cdot \frac{2P_1}{\alpha} \left( a_{\nu,k} + \frac{I_k}{2w - 1} \right) \right] \quad (31)$$

the formulas (8), (27) and (29) of the optical case can be used.

## V. COMPARISON

$P_1$  is the average power at the input of the head end. For comparison, optical receivers with reduced attenuation are used. In Fig. 5 the head end of a synchronous OCDMA system with WHC for 4 users is shown. It can be seen, this head end has got the attenuation  $\alpha = \alpha_1 \cdot \alpha_2 = 8$ . In the following we assume the attenuations  $\alpha$  listed in Tab. III of the head end. The values of  $\alpha$  for TDMC are theoretical, because a TDMA system

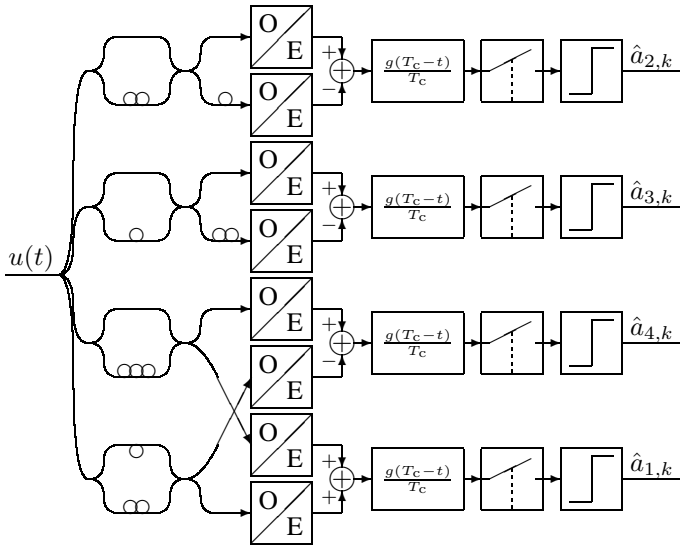


Fig. 5. Head end with reduced attenuation for synchronous OCDMA with Walsh Hadamard Code for 4 users.

TABLE III  
ASSUMED ATTENUATIONS OF THE HEAD END

TDM Code		Walsh Hadamard Code		Perfect Difference Code		
$n$	$\alpha = n$	$n$	$\alpha$	$n$	$\alpha$	$\alpha'$
2	2	2	4	3	4	4
3	3	4	8	7	10	9
4	4	8	32	13	18	8
5	5	16	32	21	30	10
6	6	32	128	31	43	18
7	7	64	128	57	78	
8	8	128	512	73	98	
9	9	256	512	91	124	
				133	179	
				183	248	

normally will be implemented with an electrical receiver with  $\alpha = 1$ . For PDC a combination of optical and electrical head end with  $\frac{\sqrt{4n-3}+1}{2}$  APDs is also possible ( $\alpha'$ ), because there are only  $\frac{\sqrt{4n-3}+1}{2}$  different receiver filters. The other filters are only delayed versions.

In all diagrams the duration  $T_c$  of one chip is the same. Thus, the bit rate of each user  $\frac{1}{nT_c}$  decreases for increasing  $n$ . The overall bitrate  $n \cdot \frac{1}{nT_c}$  of all  $n$  users together keeps constant.

All curves are calculated with the optimum decision thresholds e.g. in (16). In case of PDC the parameter  $r$  is chosen such, that the bit error probability  $P_b$  is minimized. In Fig. 6 the optimum values of  $r$  versus the power  $P_1$  at the input of the head end are plotted. The optimum  $r$  increases with increasing  $n$ .

Fig. 7 shows the bit error probability versus the power  $P_1$  at the input of the head end for TDMC and WHC. The curve for TDMC moves to the right by 3dBm if  $n$  is doubled. This is because of the attenuation of the head end (Tab. III). With WHC  $P_b$  increases much more for increasing  $n$ . Thus, optical receivers with attenuations listed in Tab. III are not feasible for

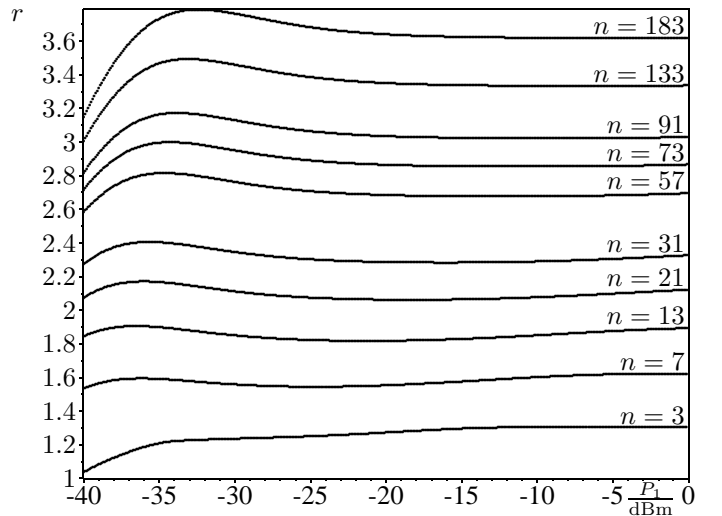


Fig. 6. Optimum parameter  $r$  versus power  $P_1$  at head end input for various numbers  $n$  of transmitter

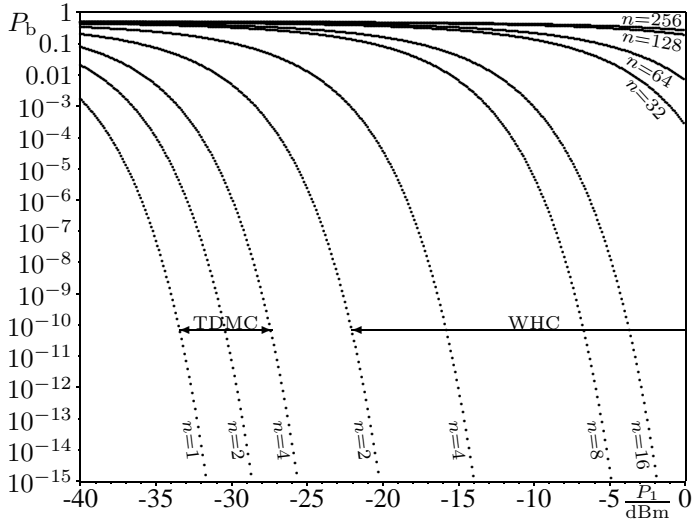


Fig. 7. Bit Error Probability  $P_b$  of TDM Codes and Walsh Hadamard Codes (WHC) versus power  $P_1$  at head end input for various numbers  $n$  of transmitter and optical decoding.

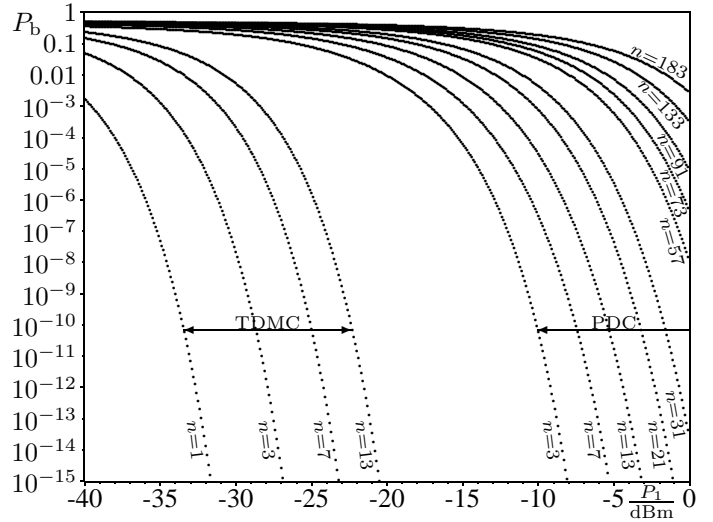


Fig. 8. Bit Error Probability  $P_b$  of TDM Codes and Perfect Difference Codes (PDC) versus power  $P_1$  at head end input for various numbers  $n$  of transmitter and optical decoding.

systems with more than  $n = 8$  subscribers.

Fig. 8 shows  $P_b$  versus the power  $P_1$  at the input of the head end for TDMC and PDC. Note, that  $n$  differs in principle for PDC and WHC, as can be seen from Tab. I. Obviously, to achieve  $P_b \leq 10^{-10}$ , PDC requires more than about 10 dBm input power  $P_1$  compared to TDMC for  $n < 13$ . However, for  $n \geq 13$ , PDC outperforms WHC. As can be seen from Tab III, the major reason is, that the attenuation in the head end increases slower for PDC than for WHC with increasing  $n$ . However, as can be seen from Figs. 7 and 8 the performance of both, PDC and WHC with optical receivers having attenuations listed in Tab. III, is much worse compared to TDMC.

The attenuation of the head end given in Tab. III turns out to be the crucial impact on the performance. Thus, in the following a head end with a single APD at the input, followed by an A/D conversion of the total electrical signal at chip rate and a subsequent digital processing is investigated. Of course, due to the high bandwidth of the electrical signal, this is a technological challenge.

Fig. 9 shows the bit error probability  $P_b$  versus the power  $P_1$  at the input of the head end for TDMC, WHC and PDC. With such a receiver,  $P_b$  for TDMC is independent of the number  $n$  of transmitters. The curve is identical with the optical receiver in Fig. 7 and Fig. 8 for  $n = 1$ . TDMC again outperforms the other synchronous OCDMA codes. As can be seen, WHC is still superior to PDC for a small number of transmitters  $n \leq 4$ . With the electrical receiver a reasonable  $P_b \leq 10^{-10}$  is reached with a much smaller input power  $P_1$ .

## VI. CONCLUSIONS

We have investigated the performance of three synchronous multiplexing schemes which can make access to a Passive Optical Network (PON): Optical TDMA (OTDMA) and optical CDMA (OCDMA) with Walsh Hadamard Codes and Perfect Difference Codes. In optical CDMA we are faced with the fact, that optical power signals are always positive, and thus the orthogonality relation cannot be fulfilled precisely. To mitigate

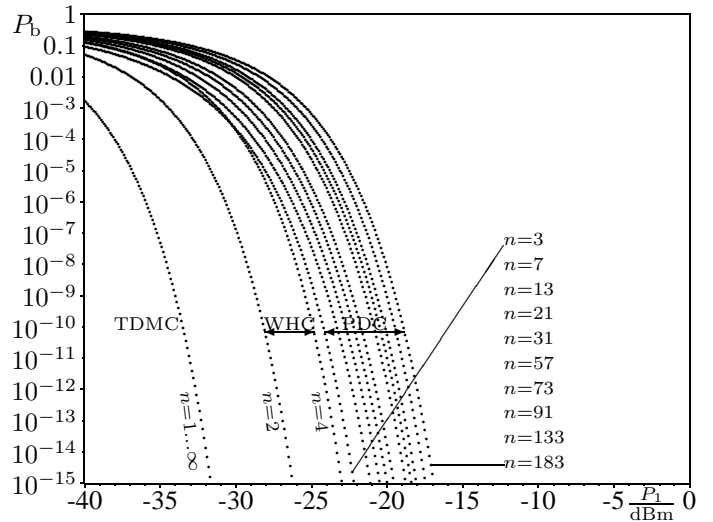


Fig. 9. Bit Error Probability  $P_b$  of TDMC, WHC and PDC versus power  $P_1$  at head end input for various numbers  $n$  of transmitter and electrical decoding.

this effect, we propose special codes for bit 1 and bit 0 which allow for differential decoding at the optical receiver. As a result, multi user interference (MUI) is reduced to zero. The different codes have been compared with respect to bit error probability and the number of transmitters allowed, in the presence of additive white Gaussian noise. Both, electrical and optical decoders have been studied. We have shown, that TDMA, either optical or electrical, performs best. This also holds, if electrical decoders are used by the other schemes. Our proposed Walsh Hadamard Code outperforms the Perfect Difference Code in case of a small number of transmitters up to about 8. The significant performance gap between electrical and optical decoding results from the fact, that (passive) power splitters are used for optical decoders, which reduce the available power at each decoder. Thus, the signal to noise ratio is lowered and consequently the bit error probability is increased. This will change, if the power loss due to the splitters is compensated by an optical amplifier at the

expense of an increased noise level. We have considered exclusively synchronous access schemes. However, it should be noted finally, that asynchronous OCDMA shows advantages, if additional transmitters have to be added to a given access network without the execution of complicated ranging procedures.

## VII. ACKNOWLEDGEMENT

Parts of this study were carried out within the FMS-Project (Forschungsverbund Medientechnik Südwest). The financing by the ministries of Baden-Württemberg and Rheinland-Pfalz is gratefully acknowledged.

## REFERENCES

- [1] Fan R. K., Chung, Jawad A. Salehi, Victor K. Wei, *Optical Orthogonal Codes: Design Analysis, and Applications*, IEEE Transactions on Information Theory, vol. 35, no. 3, May 1989.
- [2] Jawad A. Salehi, *Code Division Multiple-Access Techniques in Optical Fiber Networks - Part I: Fundamental Principles*, IEEE Transactions on Communications, vol. 37, pp. 824-833, August 1989.
- [3] Jawad A. Salehi, Charles A. Brackett, *Code Division Multiple-Access Techniques in Optical Fiber Networks - Part II: Systems Performance Analysis*, IEEE Transactions on Communications, vol. 37, pp. 834-842, August 1989.
- [4] A.F. Mohammed, *Near-far problem in direct-sequence code-division multiple-access systems*, Seventh IEEE European Conference on Mobile and Personal Communications, pp. 151-154, Dec. 1993
- [5] Roman Dischler, *FMS Projekt III.3: Digitale Übertragungsverfahren in hybriden Teilnehmerzugangsnetzen; Arbeitsbereich: Optisches CDMA als Mehrfachzugriffsverfahren für Rückkanäle in optischen Verteilnetzen im Teilnehmerzugangsbereich*, <http://www.inue.uni-stuttgart.de/FMS-Intern/Berichte/Projekt.III.3/fms33-02.pdf>; 31. März 1998
- [6] John G. Proakis, *Digital Communications*, 4th ed. 2001, pp. 424-425
- [7] Chi-Shun Weng, Jingshown Wu, *Perfect Difference Codes for Synchronous Fiber-Optic CDMA Communication Systems*, Journal of Lightwave Technology, vol. 19, no. 2, pp. 186-194, February 2001